Subscriber access provided by - Access paid by the I UC Berkeley Library

Article

A Mechanical Actuator Driven Electrochemically by Artificial Molecular Muscles

Bala Krishna Juluri, Ajeet S. Kumar, Yi Liu, Tao Ye, Ying-Wei Yang, Amar H. Flood, Lei Fang, J. Fraser Stoddart, Paul S. Weiss, and Tony Jun Huang

ACS Nano, **2009**, 3 (2), 291-300• DOI: 10.1021/nn8002373 • Publication Date (Web): 30 January 2009

Downloaded from http://pubs.acs.org on May 14, 2009

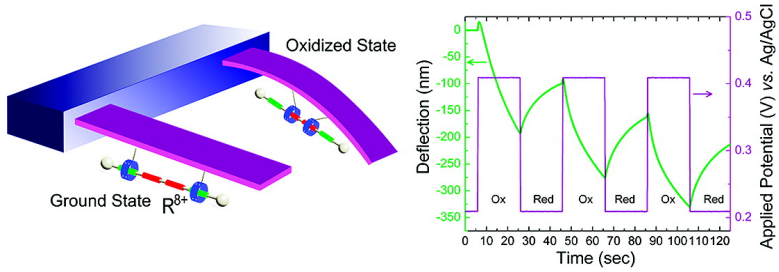

More About This Article

Additional resources and features associated with this article are available within the HTML version:

- Supporting Information
- Access to high resolution figures
- Links to articles and content related to this article
- Copyright permission to reproduce figures and/or text from this article

View the Full Text HTML

ACS Publications
High quality. High impact.

ACS Nano is published by the American Chemical Society. 1155 Sixteenth Street N.W., Washington, DC 20036

A Mechanical Actuator Driven Electrochemically by Artificial Molecular Muscles

Bala Krishna Juluri,[†] Ajeet S. Kumar,[‡] Yi Liu,[§] Tao Ye,[‡,#] Ying-Wei Yang,[⊥] Amar H. Flood,[∥] Lei Fang,[¶] J. Fraser Stoddart,[¶,*] Paul S. Weiss,[‡,*] and Tony Jun Huang[†,*]

[†]Department of Engineering Science and Mechanics, The Pennsylvania State University, University Park, Pennsylvania 16802-6812, [‡]Departments of Chemistry and Physics, The Pennsylvania State University, University Park, Pennsylvania 16802-6300, [§]The Molecular Foundry, Lawrence Berkeley National Laboratory, Berkeley, California 94720, [⊥]Department of Chemistry and Biochemistry, University of California, Los Angeles, 405 Hilgard Avenue, Los Angeles, California 90095-1569, [∥]Department of Chemistry, Indiana University, Bloomington, Indiana 47405-7102, and [¶]Department of Chemistry, Northwestern University, 2145 Sheridan Road, Evanston, Illinois 60208-3111. [#]Present address. School of Natural Sciences, University of California, Merced, California 95344.

ABSTRACT A microcantilever, coated with a monolayer of redox-controllable, bistable [3]rotaxane molecules (artificial molecular muscles), undergoes reversible deflections when subjected to alternating oxidizing and reducing electrochemical potentials. The microcantilever devices were prepared by precoating one surface with a gold film and allowing the palindromic [3]rotaxane molecules to adsorb selectively onto one side of the microcantilevers, utilizing thiol-gold chemistry. An electrochemical cell was employed in the experiments, and deflections were monitored both as a function of (i) the scan rate ($\leq$20 mV s^{-1}) and (ii) the time for potential step experiments at oxidizing ($>+0.4$ V) and reducing ($<+0.2$ V) potentials. The different directions and magnitudes of the deflections for the microcantilevers, which were coated with artificial molecular muscles, were compared with (i) data from nominally bare microcantilevers precoated with gold and (ii) those coated with two types of control compounds, namely, dumbbell molecules to simulate the redox activity of the palindromic bistable [3]rotaxane molecules and inactive 1-dodecanethiol molecules. The comparisons demonstrate that the artificial molecular muscles are responsible for the deflections, which can be repeated over many cycles. The microcantilevers deflect in one direction following oxidation and in the opposite direction upon reduction. The ~550 nm deflections were calculated to be commensurate with forces per molecule of ~650 pN. The thermal relaxation that characterizes the device's deflection is consistent with the double bistability associated with the palindromic [3]rotaxane and reflects a metastable contracted state. The use of the cooperative forces generated by these self-assembled, nanometer-scale artificial molecular muscles that are electrically wired to an external power supply constitutes a seminal step toward molecular-machine-based nanoelectromechanical systems (NEMS).

KEYWORDS: bistable rotaxanes · electrochemistry · microcantilever · molecular machines · NEMS · supramolecular chemistry

Inspired by the inherent promise and opportunities in nanotechnology, the scientific community has been attempting to decrease the characteristic length scales that define mechanical, electronic, and other devices.[1,2] A wide range of applications, including robotic, optical, and microfluidic systems, call for microscale and nanoscale actuators.[3] Most conventional electrostatic and piezoelectric materials, however, require high driving voltages, and they have to be fabricated using photolithography and other top-down manufacturing techniques that cannot easily achieve[4] feature sizes below 100 nm. In contrast, bottom-up approaches[5] that employ atoms and molecules as their fundamental building blocks and working units can potentially deliver mechanical operations on much reduced size scales.[6−9] Recently, research has been directed[10] toward developing an integrated approach that combines the functionality of bottom-up assembly with top-down techniques for the manufacture of hybrid nanoelectromechanical systems (NEMS).

A number of nanomechanical actuators[5,11−23] have been fabricated by hybrid top-down/bottom-up approaches. Electromechanical expansion in sheets of single-walled carbon nanotubes, proposed by Baughman *et al.*,[11] has resulted in microscale actuation with strains higher than those obtained using conventional ferroelectrics. The phenomenon of hydrogel swelling by radiative forces was used by Juodkazis *et al.*[12] to build light-sensitive actuators. Redox-activated electrostatic repulsion in polymer molecules, such as polyaniline[15] and polypyrrole,[16] has also been employed to power reversible actuation in microcantilevers. Raguse *et al.*[17] have utilized the intercalation of ions in nanoparticle films to achieve electrochemical actuation. These systems rely upon the bulk response of materials, and recently, researchers have started to harness work from molecular-scale mechanical motions. For example, Shu *et al.*[19] demonstrated the controlled, reversible actuation of a microcantilever, using pH-controlled

*Address correspondence to stoddart@northwestern.edu, stm@psu.edu, junhuang@psu.edu.

Received for review April 21, 2008 and accepted January 19, 2009.

Published online January 30, 2009.
10.1021/nn8002373 CCC: $40.75

© 2009 American Chemical Society

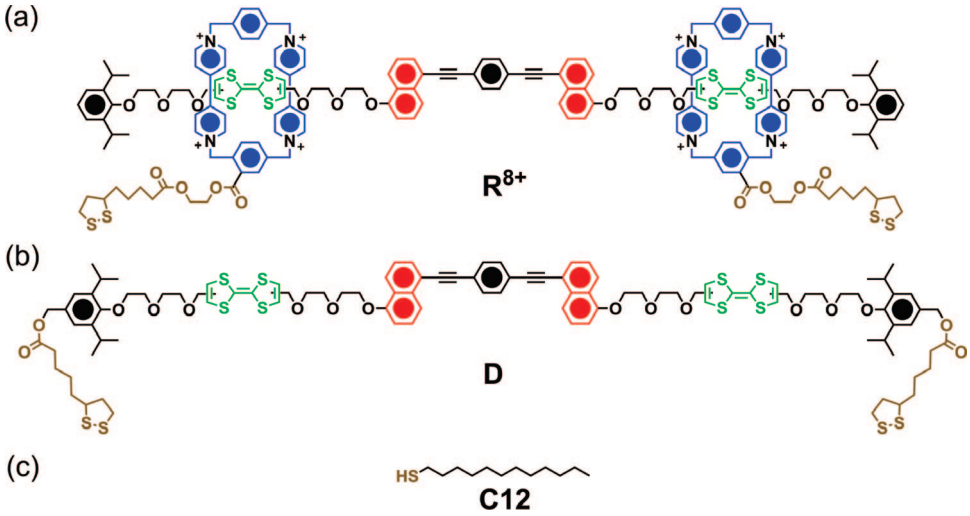

Scheme 1. Molecular structures of (a) palindromic bistable [3]rotaxane $\mathbf{R}^{8+}$, (b) disulfide-tethered dumbbell D (control compound related to $\mathbf{R}^{8+}$), and (c) 1-dodecanethiol C12 (control compound).

conformational changes (duplex to i-motif) in self-assembled monolayer (SAM) matrices of DNA. While a monolayer of a photosensitive protein complex (bacteriorhodopsin) has been employed by Thomas *et al.*[20] and Ren *et al.*[21] to actuate microcantilevers photochemically, other experimentalists[22] have exercised photochemical control upon the configurational (*cis*/*trans*) isomerization of azobenzene molecules to actuate microcantilevers.

Artificial molecular machinery[5−8,24−36] has emerged as one of the most attractive alternatives for performing controllable mechanical work that begins at the nanoscale. These molecular machines have proven to be integral to the operation and performance of many nanoscale and microscale systems, including molecular electronics,[9,26,37−47] nanovalves for drug delivery,[48−53] tunable electrochromic devices,[54−58] as well as light-powered devices for transporting liquid over millimeters[59] and for rotating microscale objects.[60] The class of artificial molecular switches, based on bistable rotaxanes, is especially promising.[61,62] These particular nanomachines are mechanically interlocked compounds[63] composed of a dumbbell-shaped component that is encircled by one or more ring components.[44,64] Bistable, donor−acceptor rotaxanes have many advantages as actuation materials. Most importantly, bistable rotaxanes can deliver controllable mechanical motions at the molecular level—a characteristic that most existing micro/nanoactuators[1,10−22] do not possess—and thus can be ideal for applications where ultrasmall nanoactuators are needed. In addition, (1) they can generate tunable strains (*e.g.*, up to 42%), while the strain generated[4] by traditional piezoelectric actuators is typically less than 1%;[65,66] (2) they can undergo controlled mechanical motion, following the input of a variety of external stimuli (chemical, electrochemical, and optical), while traditional actuators[3,67] and biomotors[68] usually rely on a single stimulus; and (3) bistable [2]rotaxanes also offer the synthetically tunable property of hysteretic switching by taking advantage of a metastable state.[39,54,69,70] In this manner, the molecules can persist in their actuated state long after the stimulus is removed.

We recently extended research beyond simple bistable [2]rotaxanes by designing and synthesizing a disulfide-tethered, palindromic, bistable [3]rotaxane $\mathbf{R}^{8+}$ (Scheme 1) that mimics[65,66] biological skeletal muscle's contraction and extension. Skeletal muscles convert chemical energy to mechanical energy by the cumulative actions of myosin biomotors.[71] Coherent and cooperative conformational changes in this biosystem are harnessed in order to obtain macroscopic muscle contraction and expansion.[72,73] By imitation of the changes in shape that occur in skeletal muscles, the palindromic, bistable [3]rotaxane $\mathbf{R}^{8+}$ undergoes controllable mechanical motions in the presence of external stimuli. It has a pair of redox-active tetrathiafulvalene (TTF) units, a pair of naphthalene (NP) stations separated by a di(ethylene glycol) spacer, and two movable tetracationic, cyclobis(paraquat-*para*-phenylene) ($CBPQT^{4+}$) rings (Scheme 1). In the ground-state co-conformation, both the $CBPQT^{4+}$ rings encircle the TTF units, courtesy of electron donor−acceptor interactions.[66] Oxidation of the TTF units causes the $CBPQT^{4+}$ rings to move toward the NP stations because of the electrostatic repulsion between the rings and the positively charged TTF^{2+} units. Reducing the TTF^{2+} dications back to their neutral state causes the rings to shuttle back onto the TTF units. The incorporation of a disulfide tether onto each $CBPQT^{4+}$ ring component provides a point of attachment to gold surfaces. More critically, this connection provides the means to transfer the energy of contraction within the artificial muscle molecules to an underlying substrate.

The collective motions induced by oxidation and reduction of ∼8 billion muscle molecules can be harnessed to perform mechanical work on a microcantilever.[65,66] Reversible flexing of a microcantilever coated with $\mathbf{R}^{8+}$ during the cyclic injection of oxidizing and reducing solutions was correlated to the collective contraction and extension−relaxation of the surface-bound muscle molecules. This work constituted a starting point in molecular-muscle-based NEMS. However, the introduction of different chemicals into the system

is a slow and inconvenient process that is associated with the gradual accumulation of waste products. Succinctly, chemically controlled actuation is not optimal for many engineering applications. Compared to chemical methods, electrochemically or photochemically induced oxidation and reduction have many advantages: (i) devices can be switched much faster; (ii) they can work without producing chemical waste; and (iii) either electricity or light can be used for both inducing (writing) and detecting (reading) mechanical molecular motions in devices. Here, we demonstrate the feasibility of electrochemically controlled surface-bound molecular muscles and use the collective mechanical motions of the bistable molecules to perform mechanical work on a larger scale. The electrochemically induced movements employing the rotaxane molecules bend the cantilevers in the opposite directions to those observed for the control systems, in which electrolyte adsorption appears to play the major role. We were not able to determine the exact oxidation states of the TTF units (+1 or +2) within the surface-bound rotaxanes. However, the observed thermal relaxation of the proposed metastable state ($k = 1.2 \times 10^{-2}$ s^{-1}) monitored in the device's deflection is consistent with internal movements resulting from the TTF units' oxidation in the molecules,[39,54,69,70,74] as well as the primary role of the molecular muscles in bending the microcantilevers up and down.

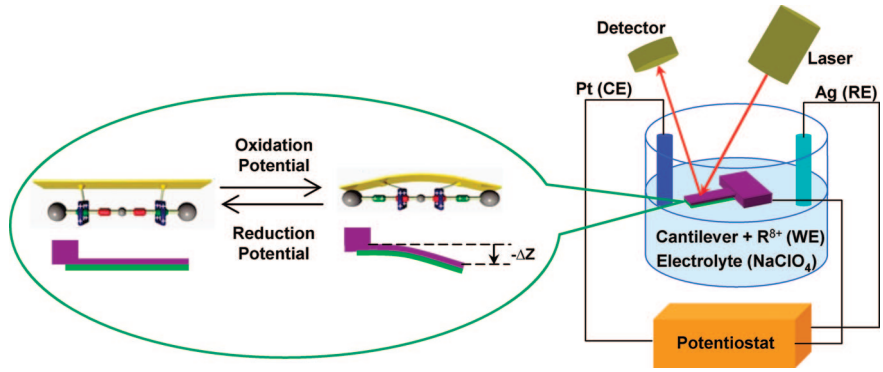

Figure 1. Schematic of the experimental setup used for *in situ* electrochemical activation of the palindromic bistable [3]rotaxane molecules. The inset shows the reversible electrochemical oxidation and reduction of $\mathbf{R}^{8+}$ to produce the microcantilever deflection (WE: working electrode, CE: counter electrode, RE: reference electrode).

RESULTS AND DISCUSSION

In order to detect the mechanical work exerted by the surface-bound, palindromic, bistable [3]rotaxane $\mathbf{R}^{8+}$ on microcantilevers during electrochemical activation, we combined (Figure 1) an optical deflection technique based on atomic force microscopy (AFM) with an *in situ* electrochemical method. A microcantilever coated on one side with gold was used as a working electrode, a silver wire as a quasi-reference electrode, and a platinum wire as a counter electrode. These three electrodes were placed in a Teflon cell filled with aqueous electrolyte (0.1 M $NaClO_4$). The silver wire pseudo-reference electrode was subsequently calibrated against a Ag/AgCl 3 M KCl reference. The data illustrated in Figures 2−4 represent the calibrated redox potentials. The gold surface of the microcantilever was coated with a monolayer film of $\mathbf{R}^{8+}$ molecules, and the redox state was changed by applying a desired potential using a potentiostat (CHInstrument, Inc.). A laser beam reflected by the silicon side of the microcantilever was collected by a split photodiode. The deflections in the microcantilever during electrochemical activation of the muscle molecules were measured from the variations in the reflected laser beam position on the photodiode.

Previously, redox-activated mechanical switching of $\mathbf{R}^{8+}$ molecules in solution was characterized extensively using cyclic voltammetry and UV−visible spectroelectrochemistry.[66] When $\mathbf{R}^{8+}$ molecules are attached onto surfaces, our expectation is that, upon the application of a sufficiently oxidizing potential, the TTF units in $\mathbf{R}^{8+}$ will become positively charged, causing the surface-bound rings to move toward the NP units. Consequently, this action will increase the bending moment of the supporting microcantilever. A reducing potential will regenerate the neutral TTF units, causing the rings to move back to these TTF units. The deflection in the microcantilever would then decrease. Therefore, by applying an electrochemical potential, it will be possible to harness the collective mechanical motions from surface-bound molecular muscles and to control the deflection of the microcantilever.

To describe the direction of the microcantilever deflection, we use the terms "down" for deflection of the microcantilever toward the gold side (negative deflection) and "up" for deflection away from the gold side (positive deflection). To determine the mechanical work exerted by molecular muscles on the microcantilevers, all competing forces acting against the mechanical work performed by molecular muscles should be low in magnitude or, ideally, nonexistent. Such competing forces, however, do exist in microcantilevers during electrochemical activation. They include electrostatic repulsion forces at solid−liquid interfaces and surface stress induced by specific adsorption and desorption of ionic species in the electrolyte.[75] To assess the influence of these competing forces, we subjected a nominally bare gold-precoated microcantilever without a molecular muscle monolayer film to a sweep of triangular potential. Figure 2a shows the performance of a bare microcantilever subjected to anodic and cathodic sweeps of electrochemical potential at a slow scan rate of 2 mV/s. The bare microcantilever was deflected upward during the anodic sweep and deflected back

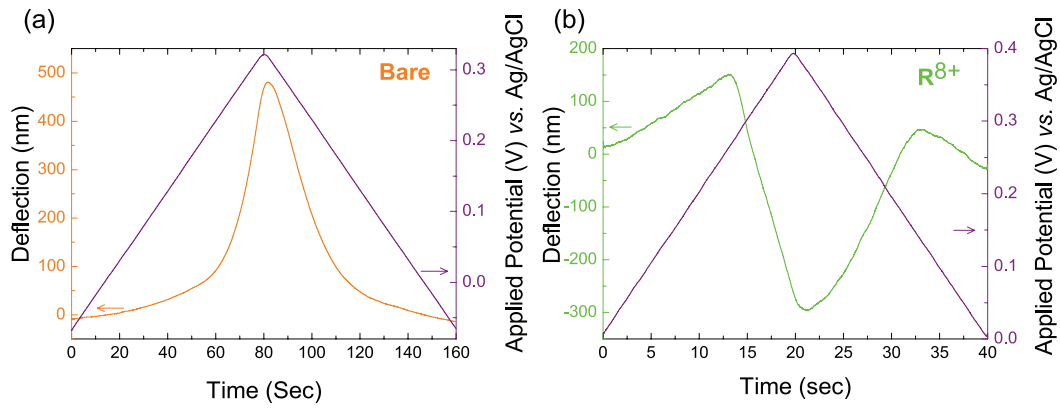

Figure 2. Deflection signature (colored lines) in response to a triangular sweep (purples lines) of the electrochemical potential for (a) bare microcantilever (orange line, 5 mV s^{-1}) and (b) microcantilever modified with a monolayer film of the palindromic bistable [3]rotaxane $\mathbf{R}^{8+}$ (green line) on one side of the microcantilever (20 mV s^{-1}). The directions of the arrows indicate the corresponding *y*-axis of the parameter plotted.

down again to the neutral position during the cathodic one. On the basis of the magnitudes of surface stress reported in earlier work,[75−78] we attribute this deflection signature to the specific adsorption of perchlorate (ClO_4^-) counterions onto the gold-coated side of the microcantilever.

We expected that, upon the oxidation of the TTF units and the consequent contraction of the distance between the rings, the collective moments of deflection caused by the many muscle molecules would flex the microcantilever (Figure 1) in the negative direction, that is, *opposing* the competing effect (Figure 2a) of specific adsorption by perchlorate counterions. *Both* effects were observed (Figure 2b) in triangular sweep experiments performed on a microcantilever coated with a monolayer film of $\mathbf{R}^{8+}$ molecules. During the anodic sweep, the initial deflection went upward. However, after reaching a potential of +0.24 V, the microcantilever started to deflect downward for various scan rates of applied potential (see Supporting Information, Figure S1a). The observed downward deflection was attributed to the collective motions of surface-bound muscle molecules that generate tensile stress on the microcantilevers. Subsequent application of a cathodic sweep caused the microcantilever to return to its original position. This restoration was believed to occur on account of the fact that reduction of the $TTF^{2+/+}$ units will lead to shuttling of the rings back to their original positions. When the potential went below +0.12 V, the microcantilever deflected downward, an observation that we attribute to the desorption of perchlorate counterions from the microcantilever occurring in the background. The initial deflection (when the driving potential is below +0.24 V) in the $\mathbf{R}^{8+}$-coated cantilevers, attributed to the specific ion adsorption, was higher than what was observed in bare cantilevers. This phenomenon is assigned to the presence of positive charges on $\mathbf{R}^{8+}$ that make the cantilever surface highly charged and more prone to specific adsorption than bare cantilevers. Another cantilever coated with $\mathbf{R}^{8+}$ molecules also showed similar deflection signatures for the same potential window and scan rate (see Supporting Information, Figure S1b), indicating good reproducibility of our experiments. It should also be noted that the magnitude of deflection observed here is much larger than the ones observed in our previous studies,[65,66] which utilized chemical stimuli and were likely limited by the diffusion and partial activation of the molecules.

To determine other effects that could contribute to the deflection of the cantilever, such as electron injection into the cantilever, we conducted control experiments with monolayer films composed of two different compounds. The first control compound (Scheme 1b) was a disulfide-tethered dumbbell compound **D**. This compound contains a pair of TTF and NP units with the same relative geometry as that present in $\mathbf{R}^{8+}$ and retains the redox activity of the [3]rotaxane. However, **D** lacks mechanically mobile $CBPQT^{4+}$ rings, while the disulfide tethers are attached at the two stoppers of the dumbbell. The second control compound (Scheme 1c) was 1-dodecanethiol ($C_{12}H_{26}SH$) **C12**, which lacks both moving elements and redox-active units, but which is known to form well-ordered SAMs that would thus block adsorption of other species.[79−84] Neither control compound was expected to perform mechanical work on the microcantilever, but it is expected that oxidation of **D** changes the electronic structure of the gold metal and creates tensile stresses on the cantilever. To test these hypotheses, monolayer films of the control molecules, assembled on microcantilevers, were subjected to triangular sweeps (Figure 3) at slow scan rates of 20 mV s^{-1}. The deflection for both control compounds was opposite to that observed in the case of $\mathbf{R}^{8+}$. This opposite movement indicates that the mechanically active, disulfide-tethered $CBPQT^{4+}$ rings in $\mathbf{R}^{8+}$ are essential for the redox-controlled bending of the cantilever beams. The small upward deflections of the microcantilevers coated with control compounds were attributed to the adsorption of perchlorate counterions on the gold side of the microcantilever. The potential-induced

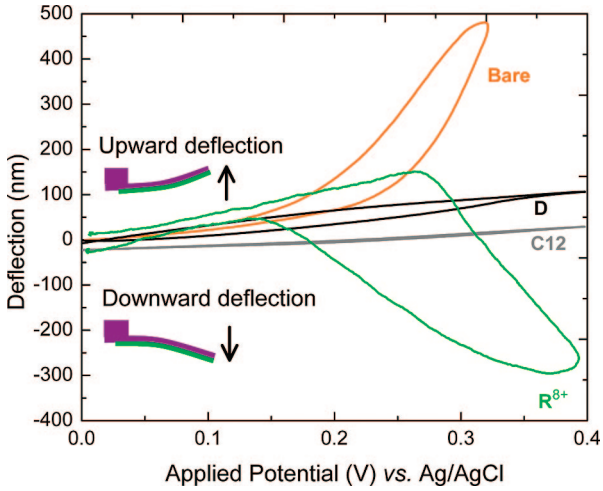

Figure 3. Deflection *versus* applied potential with respect to the working electrode for a bare microcantilever (orange line, 5 mV s^{-1}) as well as for microcantilevers coated with monolayer films of the bistable [3]rotaxane $\mathbf{R}^{8+}$ (green line, 20 mV s^{-1}), the dumbbell D (black line, 20 mV s^{-1}), and 1-dodecanethiol C12 (dark gray line, 20 mV s^{-1}).

deflections, observed for microcantilevers coated with any of the monolayers ($\mathbf{R}^{8+}$, **D**, or **C12**), were smaller in magnitude than those observed for bare microcantilevers. In these cases, the monolayers served as protective blocking layers that decreased adsorption. The adsorption for the ordered SAMs of the **C12**-coated microcantilevers was somewhat less pronounced than that observed for microcantilevers coated with **D**, as well as for those coated with $\mathbf{R}^{8+}$ prior to the onset of downward deflection. We attribute this to the ordered, dense surface packing of the **C12** SAM providing the best protection (of the films studied) from ion adsorption. The upward deflection, in the case of **D**-coated microcantilevers, suggests that the effects from specific ion adsorption dominate over the tensile stresses induced by the injection of electrons into the cantilever.

We have also performed dynamic studies in which the potential steps were alternated on a microcantilever coated with molecular muscles (Figure 4a) in order to initiate oxidation and reduction, and the deflections were measured as a function of time. On the basis of the observed deflection curves (Figure 3), the voltages of +0.4 and +0.2 V were selected in order to effect the TTF unit's oxidation and reduction, respectively. It was observed that at +0.4 V, the microcantilever deflects downward, and at a lower potential, +0.2 V, where TTF is reduced to its neutral state, the microcantilever is deflected upward. The alternate bending down and up of the microcantilever corresponds to the alternate oxidation and reduction of the surface-coated muscle molecules, respectively. We applied similar alternating potential steps to other microcantilevers, coated with either the control compounds **D** or **C12**. The cantilevers bent upward during the application of a higher potential step and bent downward during the application of a lower potential step (Figure 4b,c). Both deflections were in the opposite directions to those observed (Figure 4a) for the $\mathbf{R}^{8+}$-coated microcantilevers.

When we repeated the redox chemistry, we observed (Figure 4a) a gradual downward deflection of the cantilever. This overlying strain effect, or creep,[85] has been observed in other electrochemical actuator systems.[86−90] The creep in these systems is purportedly caused by the disentanglement of the adsorbed molecular components.[87,90] We believe that a similar creep mechanism may apply here but, in our case, arising from a reorganization of the muscle molecules within the monolayer film that plays an important role during the electrochemical perturbation. Similar behavior—the gradual deflection toward the coated side of the cantilever—was also observed in the microcantilevers coated with **D** (Figure 4b) and **C12** (Figure 4c). However, such behavior was not observed in experiments (data not shown) conducted on bare microcantilevers. These observations are consistent with our hypothesis on the creep mech-

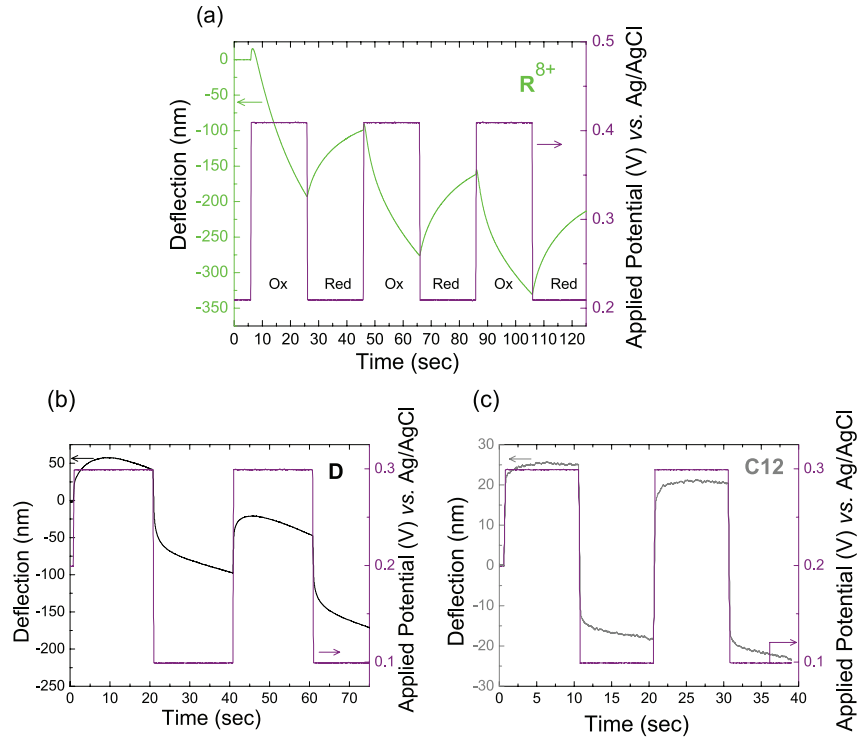

Figure 4. Time-dependent operation of microcantilevers coated with (a) the palindromic bistable [3]rotaxane $\mathbf{R}^{8+}$ (green line), (b) the dumbbell D (black line), and (c) 1-dodecanthiol C12 (dark gray line), when subjected to a series of oxidation and reduction potential steps (purple lines).

anism. The creep of microcantilevers coated with **C12** was substantially less pronounced than that for **D**- or $\mathbf{R}^{8+}$-coated microcantilevers. One would expect molecules such as **C12**, which form more organized monolayer films, to experience far less reorganization. We further note that recent investigations have indicated the importance of the substrate atoms in thiolate motion on gold, so that we may also expect substrate atoms to move when substantial molecular forces are applied.[91−93]

The deflections of the cantilever caused by the two competing effects (anion adsorption and electron transfer into the cantilever) can be estimated from the response of the **D**-coated cantilevers. The dumbbell molecule **D** is similar to $\mathbf{R}^{8+}$, except for lacking the moving rings. Figure 3 indicates that the expected deflections from the two competing effects reach maximum deflections of ~250 nm in the upward direction. Therefore, experimentally, the total deflection produced by the muscle contraction alone can be estimated to be ~550 nm (Figure S1, Supporting Information).

We attempted to quantify the magnitude of the deflection observed analytically in the microcantilever coated with $\mathbf{R}^{8+}$ using cantilever mechanics. The deflection, Δz, caused by the collective contractions and extensions of molecular muscles can be quantified using a special case of Euler−Bernoulli's beam equation, which includes a moment at the free end of the beam, and is given by

$$\Delta z = \frac{M_{\text{beam}} \cdot L^2}{2E' I}$$

where M_{beam} is the collective deflection moment on the beam; L is the total length of the beam (450 μm, considering the effect of laser spot diameter); E' is the biaxial Young's modulus of the microcantilever (additional stiffness due to Au and $\mathbf{R}^{8+}$ monolayer is neglected) and is given by $E/(1 - \nu)$, where E is Young's Modulus (187.5 GPa) and ν is the Poisson's ratio (0.182);[94] and I is the area moment of inertia of the beam's cross section. The spacer, di(ethylene glycol), between the two DNP sites provides a semirigid character to the molecule. In an idealized model for quantitative analysis, we assume that the molecular muscles are rigid and the interactions between neighboring molecules are negligible. With these assumptions, the collective deflection moment of the beam is given by

$$M_{\text{beam}} = N \cdot 2 \cdot P \cdot (t/2) \cdot f_1 \cdot f_2 \cdot f_3$$

where N is the total number of molecules adsorbed along the width of the microcantilever; P is the Coulombic repulsion force causing the ring to move away from the TTF unit; t is the beam thickness (1 μm); f_1 is the surface coverage factor; and f_2 and f_3 are the constants corresponding to the idealized geometry and the molecule's orientation, respectively (assumed to be random). Since only the molecular segment between the two rings generated a moment that contributed to the deflection, $f_2 = L_1/L_2$, where L_1 is the length between two rings at their starting positions and L_2 is the total length of the molecule. For a molecule in its extended inter-ring co-conformation, L_1 was 4.2 nm and L_2 was 7.4 nm.[66] With the molecules and deposition protocol employed, we do not expect all the molecules to be fully extended; thus L_1 and L_2 would vary and they could each be smaller than indicated above. Since the molecules were randomly aligned and only the force exerted along the longitudinal axis of the beam will contribute to deflection, $f_3 = 2/\pi$. The number of molecules along the width was approximated as w/b, where b was the breadth of each rotaxane (1 nm) and w was the breadth of the cantilever (100 μm). The success of the model to quantify the deflection observed in the experiments lies in the ability to predict the repulsion force between $CBPQT^{4+}$ ring and the TTF^{2+} station accurately. Assuming the TTF unit is oxidized to TTF^{2+} and neglecting the effects of (1) electrolyte, (2) presence of counteranions, and (3) orientation of the molecules, we can use the actuation energetics of a similar molecule reported by Brough *et al.*[95] By augmenting the force spectroscopy data with molecule dynamics simulations and considering the effects of thermal fluctuations as a function of the probe's loading rate, they were able to predict the actuation energy, W, between TTF^{2+} and $CBPQT^{4+}$. A value of 65 kcal/mol was determined to be the actuation energy, a value that also matches with *ab initio* calculations. To convert actuation energy, W, to average actuation force, P, we divide W by the distance between TTF^{2+} and DNP, $d = 1.4$ nm, giving a value of 320 pN. Using this magnitude for the force and assuming a surface coverage of 100%, the theoretical displacement was predicted to be 620 nm. This value is slightly larger than the magnitude of deflection (~550 nm) observed in the experiments, but well within the accuracy of various assumptions made in the model.

The first cycle of oxidation and reduction caused a larger deflection than did subsequent cycles. The extent of the deflection stabilized (Figure 5) after the first cycle. We attribute the sudden changes in the downward and upward deflection at the end of the first cycle to the incomplete recovery of the ground-state coconformation from the metastable state coconformation,[39,54,69,70] which leaves only a portion of the muscle molecules active for subsequent cycles. This observation suggested that a microcantilever, if left in a reducing environment after a series of oxidation and reduction cycles, should have most of the surface-bound rotaxane molecules recover to their ground-state co-conformation. With a new set of actuation cycles, the first cycle would once again exhibit large changes in downward and upward deflection.

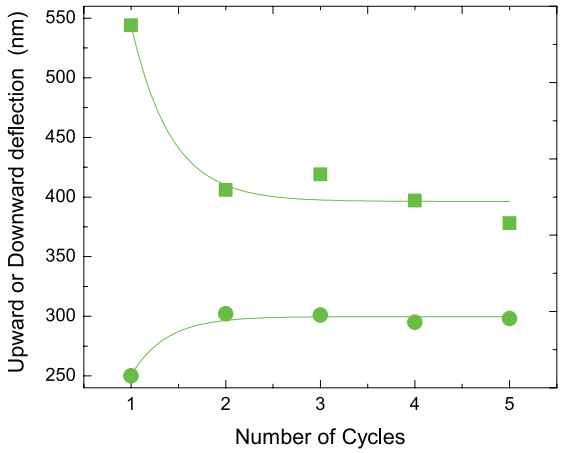

Figure 5. Comparison of the downward deflection as a result of the application of an oxidizing potential (squares) and the upward deflection caused by the application of reducing potential (circles) in a microcantilever modified with a bistable [3]rotaxane $\mathbf{R}^{8+}$ monolayer film followed through five actuation cycles. Solid lines represent the best fits.

To test this hypothesis, we applied three stages of potential variations (Figure 6) while the cantilever deflection was recorded. Stage I included seven steps of alternating oxidation and reduction potentials with 20 s intervals at each potential for each step. During these steps, the microcantilever bent alternately downward and upward, as expected for these artificial molecular muscles. Large changes in the downward and upward deflections were observed in the first cycle of actuation, followed by constant upward and downward deflections in the following actuation cycles. Sudden changes or "spikes" in the deflection of the microcantilever were observed at the end of each oxidation and reduction stage. These spikes most likely resulted from desorption and adsorption of the perchlorate counterions. In

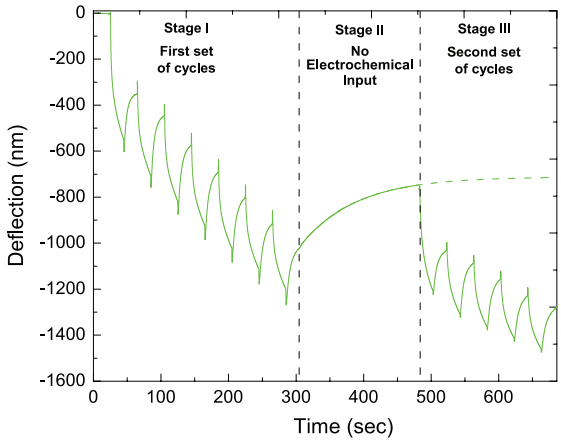

Figure 6. Actuation of a microcantilever coated with $\mathbf{R}^{8+}$ molecules when subjected to three types of electrochemical potential variations. In Stage I, seven steps of alternating oxidizing and reducing potentials were applied. In Stage II, no external potential was applied for 175 s. This period enabled recovery of the cantilever, as noted from the fit (dotted line) of the deflection signature observed in Stage II. In Stage III, five steps of alternating oxidizing and reducing potentials were applied.

Stage II, the microcantilever was left electrochemically unperturbed at an open circuit potential—that is, no potential applied—for ~175 s. During this stage, the cantilever deflected upward with a first-order decay ($k = 0.012\ s^{-1}$). The recovery of the cantilever position appeared to be incomplete, possibly as a result of the irreversible creep observed in Stage I. A time interval of 175 s was chosen for Stage II in order to ensure saturation of the recovery process. In Stage III, we again applied alternating redox potentials with the same durations as those applied in Stage I. We observed deflection signatures similar to those in Stage I. Large changes in the downward and upward deflections were again observed in the first cycle of operation. These changes were followed by constant upward and downward deflections in later cycles within the error of our measurements.

The observation of an exponential decay for the relaxation of the $\mathbf{R}^{8+}$-coated microcantilever's deflection curve is consistent with the behavior of bistable [2]rotaxanes in solution,[70,74] embedded in polymer matrices,[54] and self-assembled onto gold surfaces.[69] In these previous cases, the relaxations of the molecules were observed directly using electrochemistry, and it was found that the rates of motion slowed down[39,70] as the rotaxanes were transferred into more highly condensed phases. Their kinetic behavior was found to correlate with the thermal relaxation of the electrical signature from a device that has rotaxanes incorporated within them as Langmuir–Blodgett monolayers.[39,70] We posit, therefore, that the first-order decay in the deflection of the microcantilever arises from the thermally activated motion of the mobile rings from the NP stations back to the neutral TTF stations. The rate constant correlates with an activation barrier of $\Delta G = 20$ kcal mol^{-1}. On the basis of solution-phase studies[66] on the molecular muscle prototype to $\mathbf{R}^{8+}$, the corresponding barrier was estimated to be less than 14 kcal mol^{-1}. Consequently, there is an increase of 6 kcal mol^{-1} on going from solution to surface-bound devices. This increase is greater than the ~2 kcal mol^{-1} expected on the basis of the bistable rotaxane studied, first in solution, and then self-assembled onto gold electrodes. Slower than usual thermal relaxation has been observed for the *cis*-to-*trans* isomerization[96] in single polymer strands incorporating multiple azobenzene units when these strands are placed under loads by utilizing microcantilevers in force spectroscopy experiments. We concur with the rationalization presented in this previous report that the load-induced motion is no longer able to proceed along the lowest pathway possible. The exponential decay arises either when configurationally active molecules (azobenzene) or when active rotaxanes with two mobile rings ($\mathbf{R}^{8+}$) relax in confluence with an applied restoring force. The data suggest that the active units are not interacting with each other. Nevertheless, the observation of a relaxation process is a crucial molecular

signature that confirms the dominant role that the surface-bound rotaxanes serve in bending the microcantilevers.

CONCLUSIONS AND OUTLOOK

We have demonstrated that surface-bound artificial muscle molecules, when electrochemically activated, cause a microcantilever to bend. Conversely, microcantilever beams that are coated with redox-active but mechanically inert control compounds—the dumbbell of the [3]rotaxane or 1-dodecanethiol—do not display the same bending characteristics. Moreover, using beam theory and analysis, it has been shown that these observations are consistent with the hypothesis that the cumulative nanoscale movements of the surface-bound "molecular muscles" can be activated electrochemically and harnessed to perform much larger-scale mechanical work. The observed "creep" phenomenon in the dynamic studies most likely results from the reorganization of the molecules in the films. Compared with their chemically driven counterparts,[65,66] the electrochemically driven molecular-muscle-based actuators can be operated much faster, more conveniently, and with larger responses. We also recognize that due to the significant complexity in the dynamic molecular switching behavior on solid substrates, many fundamental questions remain to be answered. We believe that (i) by improving the assembly conditions, (ii) by increasing the rigidity of the muscle molecules, and (iii) by incorporating a blocking layer in a matrix around the active components, the artificial molecular-muscle-based NEMS can be understood and optimized further. Nevertheless, the results constitute significant advances over prior efforts and a key step toward functional NEMS based on artificial molecular muscles.

MATERIALS AND METHODS

Preparation of Microcantilever Samples. Commercial rectangular silicon microcantilevers (NanoAndMore Inc., Lady's Island, SC) of length 500 μm, width 100 μm, and thickness 1 μm were used in all the experiments. One side of the microcantilevers was coated with a 20 nm thick gold layer by the manufacturer. Before a monolayer film was deposited, each microcantilever was cleaned for 5 min with UV/ozone and then washed with DI water.

Synthesis of Molecular Muscles and Control Compounds and Preparation of Monolayer Films. The palindromic bistable [3]rotaxane $\mathbf{R}^{8+}$ and the control dumbbell compound **D** were synthesized using a method reported earlier.[49,66] 1-Dodecanethiol, **C12** (Sigma-Aldrich), was used without further purification. Microcantilevers were cleaned and then placed for 48 h in solutions containing the target molecule in order to form monolayer films on the gold layers.

Electrochemical Atomic Force Microscope Cell. A scanning probe microscope, combined with an electrochemical cell supply (Pico SPM 2500, Molecular Imaging), was used in all of the experiments. Before each experiment, the electrolyte (0.1 M $NaClO_4$) employed in the electrochemistry setup was purged with nitrogen gas. Both counter and reference electrodes were cleaned by ultrasonication in water and acetone before each experiment. At the end of each experiment, the potential of the reference electrode (Ag) was adjusted with respect to that of a AgCl solution. The sensitivity of each microcantilever was calibrated by fitting the slopes of force curves in order to measure the cantilever deflection (nm) by means of the photodiode signal (V). The free vibration spectra and the power spectrum density were obtained using a spectrum analyzer. The spectra were fit to Lorentzian forms around the angular resonance frequency, and the spring constant of each individual cantilever was calculated from the geometry and angular resonance frequency. The deflection data and applied voltage signal were obtained with 2 ms time resolution and were later averaged from 100 data points. The signals were analyzed and plotted using MATLAB 7.0 (The Mathworks, Natick, MA) and Origin Pro (Origin Laboratory Co., Northampton, MA).

Acknowledgment. This work was supported by the Air Force Office of Scientific Research (FA9550-08-1-0349), the Penn State Center for Nanoscale Science (MRSEC), and a Nanoscale Interdisciplinary Research Team (NIRT) grant from the National Science Foundation (ECCS-0609128, ECCS-0801922). The authors thank Vin Crespi, Xiaole Mao, T. J. Mullen, Jinjie Shi, Thomas R. Walker, and Yuebing Zheng for helpful discussions. Y.L. acknowledges the support by the Office of Science, Office of Basic Energy Sciences, of the U.S. Department of Energy under Contract No. DE-AC02-05 CH11231.

Note added after ASAP publication: In the version posted January 30, 2009, incorrect versions of Figures 1 and 3 and the Table of Contents were published. The corrected version was reposted February 6, 2009.

Supporting Information Available: Additional experimental data on the effects of the potential scan rate and the reproducibility of deflection, as well as details of the estimate of deflection due to the artificial muscle molecules alone. This material is available free of charge *via* the Internet at http://pubs.acs.org.

REFERENCES AND NOTES

1. Lyshevski, S. E. *Nano-and Micro-Electromechanical Systems: Fundamentals of Nano- and Microengineering*; CRC Press: Boca Raton, FL, 2005.
2. Ozin, G. A.; Manners, I.; Fournier-Bidoz, S.; Arsenault, A. Dream Nanomachines. *Adv. Mater.* **2005**, *17*, 3011–3018.
3. Liu, C. *Foundations of MEMS*; Pearson Education: Upper Saddle River, NJ, 2006.
4. Gianchandani, Y.; Tabata, O.; Zappe, H. *Comprehensive Microsystems*: Elsevier: Amsterdam, 2007.
5. Browne, W. R.; Feringa, B. L. Making Molecular Machines Work. *Nat. Nanotechnol.* **2006**, *1*, 25–35.
6. Feringa, B. L. The Art of Building Small: From Molecular Switches to Molecular Motors. *J. Org. Chem.* **2007**, *72*, 6635–6652.
7. Baranoff, E.; Barigelletti, F.; Bonnet, S.; Collin, J.-P.; Flamigni, L.; Mobian, P.; Sauvage, J.-P. From Photoinduced Charge Separation to Light-Driven Molecular Machines. *Struct. Bonding (Berlin)* **2007**, *123*, 41–78.
8. Kay, E. R.; Leigh, D. A.; Zerbetto, F. Synthetic Molecular Motors and Mechanical Machines. *Angew. Chem., Int. Ed.* **2007**, *46*, 72–191.
9. Green, J. E.; Choi, J. W.; Boukai, A.; Bunimovich, Y.; Johnston-Halperin, E.; Delonno, E.; Luo, Y.; Sheriff, B. A.; Xu, K.; Shin, Y. S.; Tseng, H.-R.; Stoddart, J. F.; Heath, J. R. A 160-Kilobit Molecular Electronic Memory Patterned at 10^{11} Bits Per Square Centimetre. *Nature* **2007**, *445*, 414–417.
10. Craighead, H. G. Nanoelectromechanical Systems. *Science* **2000**, *290*, 1532–1535.
11. Baughman, R. H.; Cui, C. X.; Zakhidov, A. A.; Iqbal, Z.; Barisci, J. N.; Spinks, G. M.; Wallace, G. G.; Mazzoldi, A.; De Rossi, D.; Rinzler, A. G.; Jaschinski, O.; Roth, S.; Kertesz, M.

Carbon Nanotube Actuators. *Science* **1999**, *284*, 1340–1344.
12. Juodkazis, S.; Mukai, N.; Wakaki, R.; Yamaguchi, A.; Matsuo, S.; Misawa, H. Reversible Phase Transitions in Polymer Gels Induced by Radiation Forces. *Nature* **2000**, *408*, 178–181.
13. Fritz, J.; Baller, M. K.; Lang, H. P.; Rothuizen, H.; Vettiger, P.; Meyer, E.; Guntherodt, H. J.; Gerber, C.; Gimzewski, J. K. Translating Biomolecular Recognition into Nanomechanics. *Science* **2000**, *288*, 316–318.
14. Wu, G.; Ji, H.; Hansen, K.; Thundat, T.; Datar, R.; Cote, R.; Hagan, M. F.; Chakraborty, A. K.; Majumdar, A. Origin of Nanomechanical Cantilever Motion Generated from Biomolecular Interactions. *Proc. Natl. Acad. Sci. U.S.A.* **2001**, *98*, 1560–1564.
15. Lahav, M.; Durkan, C.; Gabai, R.; Katz, E.; Willner, I.; Welland, M. E. Redox Activation of a Polyaniline-Coated Cantilever: An Electro-Driven Microdevice. *Angew. Chem., Int. Ed.* **2001**, *40*, 4219–4221.
16. Tabard-Cossa, V.; Godin, M.; Grütter, P.; Burgess, I.; Lennox, R. B. Redox-Induced Surface Stress of Polypyrrole-Based Actuators. *J. Phys. Chem. B* **2005**, *109*, 17531–17537.
17. Raguse, B.; Muller, K. H.; Wieczorek, L. Nanoparticle Actuators. *Adv. Mater.* **2003**, *15*, 922–926.
18. Bay, L.; West, K.; Sommer-Larsen, P.; Skaarup, S.; Benslimane, M. A Conducting Polymer Artificial Muscle with 12% Linear Strain. *Adv. Mater.* **2003**, *15*, 310–313.
19. Shu, W. M.; Liu, D. S.; Watari, M.; Riener, C. K.; Strunz, T.; Welland, M. E.; Balasubramanian, S.; McKendry, R. A. DNA Molecular Motor Driven Micromechanical Cantilever Arrays. *J. Am. Chem. Soc.* **2005**, *127*, 17054–17060.
20. Braun, T.; Backmann, N.; Vogtli, M.; Bietsch, A.; Engel, A.; Lang, H.-P.; Gerber, C.; Hegner, M. Conformational Change of Bacteriorhodopsin Quantitatively Monitored by Microcantilever Sensors. *Biophys. J.* **2006**, *90*, 2970–2977.
21. Ren, Q.; Zhao, Y. P.; Han, L.; Zhao, H. B. A Nanomechanical Device Based on Light-Driven Proton Pumps. *Nanotechnology* **2006**, *17*, 1778–1785.
22. Ji, H. F.; Feng, Y.; Xu, X. H.; Purushotham, V.; Thundat, T.; Brown, G. M. Photon-Driven Nanomechanical Cyclic Motion. *Chem. Commun.* **2004**, *22*, 2532–2533.
23. Huang, T. J.; Juluri, B. K. Biological and Biomimetic Molecular Machines. *Nanomedicine* **2008**, *3*, 107–124.
24. Balzani, V.; Credi, A.; Raymo, F. M.; Stoddart, J. F. Artificial Molecular Machines. *Angew. Chem., Int. Ed.* **2000**, *39*, 3348–3391.
25. Balzani, V.; Venturi, M.; Credi, A. *Molecular Devices and Machines: A Journey into the Nanoworld*; Wiley-VCH: Weinheim, Germany, 2003.
26. Flood, A. H.; Ramirez, R. J. A.; Deng, W. Q.; Muller, R. P.; Goddard, W. A.; Stoddart, J. F. Meccano on the Nanoscale—A Blueprint for Making Some of the World's Tiniest Machines. *Aust. J. Chem.* **2004**, *57*, 301–322.
27. Huang, T. J.; Tseng, H.-R.; Sha, L.; Lu, W. X.; Brough, B.; Flood, A. H.; Yu, B. D.; Celestre, P. C.; Chang, J. P.; Stoddart, J. F.; Ho, C. M. Mechanical Shuttling of Linear Motor-Molecules in Condensed Phases on Solid Substrates. *Nano Lett.* **2004**, *4*, 2065–2071.
28. Kottas, G. S.; Clarke, L. I.; Horinek, D.; Michl, J. Artificial Molecular Rotors. *Chem. Rev.* **2005**, *105*, 1281–1376.
29. Huang, T. J.; Flood, A. H.; Brough, B.; Liu, Y.; Bonvallet, P. A.; Kang, S. S.; Chu, C. W.; Guo, T. F.; Lu, W. X.; Yang, Y.; Stoddart, J. F.; Ho, C. M. Understanding and Harnessing Biomimetic Molecular Machines for NEMS Actuation Materials. *IEEE Trans.* **2006**, *3*, 254–259.
30. Khuong, T. A. V.; Nunez, J. E.; Godinez, C. E.; Garcia-Garibay, M. A. Crystalline Molecular Machines: A Quest Toward Solid-State Dynamics and Function. *Acc. Chem. Res.* **2006**, *39*, 413–422.
31. Huang, T. J. Recent Developments in Artificial Molecular Machine-Based Active Nanomaterials and Nanosystems. *MRS Bull.* **2008**, *33*, 226–231.
32. Champin, B.; Mobian, P.; Sauvage, J. P. Transition Metal Complexes as Molecular Machine Prototypes. *Chem. Soc. Rev.* **2007**, *36*, 358–366.
33. Kay, E. R; Leigh, D. A. Beyond Switches: Rotaxane- and Catenane-Based Synthetic Molecular Motors. *Pure Appl. Chem.* **2008**, *80*, 17–29.
34. Badjic, J. D.; Balzani, V.; Credi, A.; Stoddart, J. F. A Molecular Elevator. *Science* **2004**, *303*, 1845–1849.
35. Moonen, N. N. P.; Flood, A. H.; Fernández, J. M.; Stoddart, J. F. Towards a Rational Design of Molecular Switches and Sensors from Their Basic Building Blocks. *Top. Curr. Chem.* **2005**, *262*, 99–132.
36. Badjic, J. D.; Ronconi, C. M.; Stoddart, J. F.; Balzani, V.; Silvi, S.; Credi, A. Operating Molecular Elevators. *J. Am. Chem. Soc.* **2006**, *128*, 1489–1499.
37. Heath, J. R.; Ratner, M. A. Molecular Electronics. *Phys. Today* **2003**, *56*, 43–49.
38. Mantooth, B. A.; Weiss, P. S. Fabrication, Assembly, and Characterization of Molecular Electronic Components. *Proc. IEEE* **2003**, *91*, 1785–1802.
39. Flood, A. H.; Stoddart, J. F.; Steuerman, D. W.; Heath, J. R. Whence Molecular Electronics. *Science* **2004**, *306*, 2055–2056.
40. Moore, A. M.; Dameron, A. A.; Mantooth, B. A.; Smith, R. K.; Fuchs, D. J.; Ciszek, J. W.; Maya, F.; Yao, Y.; Tour, J. M.; Weiss, P. S. Molecular Engineering and Measurements to Test Hypothesized Mechanisms in Single Molecule Conductance Switching. *J. Am. Chem. Soc.* **2006**, *128*, 1959–1967.
41. Collier, C. P.; Mattersteig, G.; Wong, E. W.; Luo, Y.; Beverly, K.; Sampaio, J.; Raymo, F. M.; Stoddart, J. F.; Heath, J. R. A [2]Catenane Based Solid-State Electronically Reconfigurable Switch. *Science* **2000**, *289*, 1172–1175.
42. Pease, A. R.; Jeppesen, J. O.; Stoddart, J. F.; Luo, Y.; Collier, C. P.; Heath, J. R. Switching Devices Based on Interlocked Molecules. *Acc. Chem. Res.* **2001**, *34*, 433–444.
43. Luo, Y.; Collier, C. P.; Jeppesen, J. O.; Nielsen, K. A.; Delonno, G.; Ho, G.; Perkins, J.; Tseng, H.-R.; Yamamoto, T.; Stoddart, J. F.; Heath, J. R. Two-Dimensional Molecular Electronics Circuits. *ChemPhysChem* **2002**, *3*, 519–525.
44. Tseng, H.-R.; Vignon, S. A.; Celestre, P. C.; Perkins, J.; Jeppesen, J. O.; Di Fabio, A.; Ballardini, R.; Gandolfi, M. T.; Venturi, M.; Balzani, V.; Stoddart, J. F. Redox-Controllable Amphiphilic [2]Rotaxanes. *Chem.—Eur. J.* **2004**, *10*, 155–172.
45. Jang, S. S.; Jang, Y. H.; Kim, Y.-H.; Goddard, W. A., III; Choi, J. W.; Heath, J. R.; Laursen, B. W.; Flood, A. H.; Stoddart, J. F.; Nørgaard, K.; Bjørnholm, T. Molecular Dynamics Simulation of Amphiphilic Bistable [2]Rotaxane Langmuir Monolayers at Air/Water Interfaces. *J. Am. Chem. Soc.* **2005**, *127*, 14804–14816.
46. Deng, W.-Q.; Flood, A. H.; Stoddart, J. F.; Goddard, W. A. Electronic Paper Display Design Based on a Tristable [2]Catenane. *J. Am. Chem. Soc.* **2005**, *127*, 15994–15995.
47. Dichtel, W. R.; Heath, J. R.; Stoddart, J. F. Designing Bistable [2]Rotaxanes for Molecular Electronic Devices. *Philos. Trans. R. Soc. London, Ser. A* **2007**, *365*, 1607–1625.
48. Nguyen, T. D.; Tseng, H.-R.; Celestre, P. C.; Flood, A. H.; Liu, Y.; Stoddart, J. F.; Zink, J. I. A Reversible Molecular Valve. *Proc. Natl. Acad. Sci. U.S.A.* **2005**, *102*, 10029–10034.
49. Nguyen, T. D.; Liu, Y.; Saha, S.; Leung, K. C.-F.; Stoddart, J. F.; Zink, J. I. Design and Optimization of Molecular Nanovalves Based on Redox-Switchable Rotaxanes. *J. Am. Chem. Soc.* **2007**, *129*, 626–634.
50. Saha, S.; Leung, K. C.-F.; Nguyen, T. D.; Stoddart, J. F.; Zink, J. I. Nanovalves. *Adv. Funct. Mater.* **2007**, *17*, 685–693.
51. Angelos, S.; Johansson, E.; Stoddart, J. F.; Zink, J. I. Mesostructured Silica Supports for Functional Materials and Molecular Machines. *Adv. Funct. Mater.* **2007**, *17*, 2261–2271.
52. Angelos, S.; Yang, Y.-W.; Patel, K.; Stoddart, J. F.; Zink, J. I. Supramolecular Nanovalves Based on Cucurbit[6]uril Pseudorotaxanes. *Angew. Chem., Int. Ed.* **2008**, *47*, 2222–2226.
53. Patel, K.; Angelos, S.; Dichtel, W. R.; Coskun, A.; Yang, Y.-W.; Zink, J. I.; Stoddart, J. F. Enzyme-Responsive Snap-Top Covered Silica Nanocontainers. *J. Am. Chem. Soc.* **2008**, *130*, 2382–2383.

54. Steuerman, D. W.; Tseng, H.-R.; Peters, A. J.; Flood, A. H.; Jeppesen, J. O.; Nielsen, K. A.; Stoddart, J. F.; Heath, J. R. Molecular-Mechanical Switch-Based Solid-State Electrochromic Devices. *Angew. Chem., Int. Ed.* **2004**, *43*, 6486–6491.
55. Deng, W. Q.; Flood, A. H.; Stoddart, J. F.; Goddard, W. A. An Electrochemical Color-Switchable RGB Dye: Tristable [2]Catenane. *J. Am. Chem. Soc.* **2005**, *127*, 15994–15995.
56. Ikeda, T.; Saha, S.; Aprahamian, I.; Leung, K. C. F.; Williams, A.; Deng, W. Q.; Flood, A. H.; Goddard, W. A., III; Stoddart, J. F. Toward Electrochemically Controllable Tristable Three-Station [2]Catenanes. *Chem. Asian J.* **2007**, *2*, 76–93.
57. Aprahamian, I.; Yasuda, T.; Ikeda, T.; Saha, S.; Dichtel, W. R.; Isoda, K.; Kato, T.; Stoddart, J. F. A Liquid-Crystalline Bistable [2]Rotaxane. *Angew. Chem., Int. Ed.* **2007**, *46*, 4675–4679.
58. Ikeda, T.; Aprahamian, I.; Stoddart, J. F. Blue-Colored Donor-Acceptor [2]Rotaxane. *Org. Lett.* **2007**, *9*, 1481–1484.
59. Berna, J.; Leigh, D. A.; Lubomska, M.; Mendoza, S. M.; Perez, E. M.; Rudolf, P.; Teobaldi, G.; Zerbetto, F. Macroscopic Transport by Synthetic Molecular Machines. *Nat. Mater.* **2005**, *4*, 704–710.
60. Eelkema, R.; Pollard, M. M.; Vicario, J.; Katsonis, N.; Ramon, B. S.; Bastiaansen, C. W. M.; Broer, D. J.; Feringa, B. L. Nanomotor Rotates Microscale Objects. *Nature* **2006**, *440*, 163.
61. Stoddart, J. F. Whither and Thither Molecular Machines. *Chem. Aust.* **1992**, *59*, 576–581.
62. Tseng, H.-R.; Vignon, S. A.; Stoddart, J. F. Toward Chemically Controlled Nanoscale Molecular Machinery. *Angew. Chem., Int. Ed.* **2003**, *42*, 1491–1495.
63. Aprahamian, I.; Miljanic, O. S.; Dichtel, W. R.; Isoda, K.; Yasuda, T.; Kato, T.; Stoddart, J. F. Clicked Interlocked Molecules. *Bull. Chem. Soc. Jpn.* **2007**, *80*, 1856–1869.
64. Jeppesen, J. O.; Nygaard, S.; Vignon, S. A.; Stoddart, J. F. Honing up a Genre of Amphiphilic Bistable [2]Rotaxanes for Device Settings. *Eur. J. Org. Chem.* **2005**, 196–220.
65. Huang, T. J.; Brough, B.; Ho, C. M.; Liu, Y.; Flood, A. H.; Bonvallet, P. A.; Tseng, H.-R.; Stoddart, J. F.; Baller, M.; Magonov, S. A Nanomechanical Device Based on Linear Molecular Motors. *Appl. Phys. Lett.* **2004**, *85*, 5391–5393.
66. Liu, Y.; Flood, A. H.; Bonvallett, P. A.; Vignon, S. A.; Northrop, B. H.; Tseng, H.-R.; Jeppesen, J. O.; Huang, T. J.; Brough, B.; Baller, M.; Magonov, S.; Solares, S. D.; Goddard, W. A.; Ho, C. M.; Stoddart, J. F. Linear Artificial Molecular Muscles. *J. Am. Chem. Soc.* **2005**, *127*, 9745–9759.
67. Kovacs, G. T. A. *Micromachined Transducers Sourcebook*; McGraw-Hill: New York, 1998.
68. Hess, H. Materials Science—Toward Devices Powered by Biomolecular Motors. *Science* **2006**, *312*, 860–861.
69. Tseng, H.-R.; Wu, D. M.; Fang, N. X. L.; Zhang, X.; Stoddart, J. F. The Metastability of an Electrochemically Controlled Nanoscale Machine on Gold Surfaces. *ChemPhysChem* **2004**, *5*, 111–116.
70. Choi, J. W.; Flood, A. H.; Steuerman, D. W.; Nygaard, S.; Braunschweig, A. B.; Moonen, N. N. P.; Laursen, B. W.; Luo, Y.; DeIonno, E.; Peters, A. J. Ground-State Equilibrium Thermodynamics and Switching Kinetics of Bistable [2]Rotaxanes Switched in Solution, Polymer Gels, and Molecular Electronic Devices. *Chem.—Eur. J.* **2006**, *12*, 261–279.
71. Goodsell, D. S. *Our Molecular Nature: The Body's Motors, Machines, and Messages*; Copernicus: New York, 1996.
72. Geeves, M. A. Stretching the Lever-Arm Theory. *Nature* **2002**, *415*, 129–131.
73. Spudich, J. A.; Rock, R. S. A Crossbridge Too Far. *Nat. Cell Biol.* **2002**, *4*, E8–E10.
74. Flood, A. H.; Peters, A. J.; Vignon, S. A.; Steuerman, D. W.; Tseng, H.-R.; Kang, S.; Heath, J. R.; Stoddart, J. F. The Role of Physical Environment on Molecular Electromechanical Switching. *Chem.—Eur. J.* **2004**, *10*, 6558–6564.
75. Ibach, H.; Bach, C. E.; Giesen, M.; Grossmann, A. Potential-Induced Stress in the Solid-Liquid Interface: Au(111) and Au(100) in an $HClO_4$ Electrolyte. *Surf. Sci.* **1997**, *375*, 107–119.
76. Tabard-Cossa, V.; Godin, M.; Beaulieu, L. Y.; Grütter, P. A Differential Microcantilever-Based System for Measuring Surface Stress Changes Induced by Electrochemical Reactions. *Sens. Actuators, B* **2005**, *107*, 233–241.
77. Quist, F.; Tabard-Cossa, V.; Badia, A. Nanomechanical Cantilever Motion Generated by a Surface-Confined Redox Reaction. *J. Phys. Chem. B* **2003**, *107*, 10691–10695.
78. Zhou, F.; Biesheuvel, P. M.; Choi, E.-Y.; Shu, W.; Poetes, R.; Steiner, U.; Huck, W. TS Polyelectrolyte Brush Amplified Electroactuation of Microcantilevers. *Nano Lett.* **2008**, *8*, 725–730.
79. Finklea, H. O.; Avery, S.; Lynch, M.; Furtsch, T. Blocking Oriented Monolayers of Alkyl Mercaptans on Gold Electrodes. *Langmuir* **1987**, *3*, 409–413.
80. Chidsey, C. E. D.; Loiacono, D. N. Chemical Functionality in Self-Assembled Monolayers: Structural and Electrochemical Properties. *Langmuir* **1990**, *6*, 682–691.
81. Alleman, K. S.; Weber, K.; Creager, S. E. Electrochemical Rectification at a Monolayer-Modified Electrode. *J. Phys. Chem.* **1996**, *100*, 17050–17058.
82. Smith, R. K.; Lewis, P. A.; Weiss, P. S. Patterning Self-Assembled Monolayers. *Prog. Surf. Sci.* **2004**, *75*, 1–68.
83. Mullen, T. J.; Dameron, A. A.; Weiss, P. S. Directed Assembly and Separation of Self-Assembled Monolayers *via* Electrochemical Processing. *J. Phys. Chem. B* **2006**, *110*, 14410–14417.
84. Nelson, J. B.; Schwartz, D. T. Electrochemical Factors Controlling the Patterning of Metals on SAM-Coated Substrates. *Langmuir* **2007**, *23*, 9661–9666.
85. Dowling, N. E. *Mechanical Behavior of Materials*; Prentice Hall: New York, 1999.
86. Herod, T. E.; Schlenoff, J. B. Doping-Induced Strain in Polyaniline: Stretchoelectrochemistry. *Chem. Mater.* **1993**, *5*, 951–955.
87. Hughes, M.; Spinks, G. M. Multiwalled Carbon Nanotube Actuators. *Adv. Mater.* **2005**, *17*, 443–446.
88. Ebron, V. H.; Yang, Z.; Seyer, D. J.; Kozlov, M. E.; Oh, J.; Xie, H.; Razal, J.; Hall, L. J.; Ferraris, J. P.; MacDiarmid, A. G.; Baughman, R. H. Fuel-Powered Artificial Muscles. *Science* **2006**, *311*, 1580–1583.
89. Mirfakhrai, T.; Oh, J.; Kozlov, M.; Fok, E. C. W.; Zhang, M.; Fang, S.; Baughman, R. H.; Madden, J. D. W. Electrochemical Actuation of Carbon Nanotube Yarns. *Smart Mater. Struct.* **2007**, *16*, S243–S249.
90. Smela, E.; Lu, W.; Mattes, B. R. Polyaniline Actuators: Part 1. PANI(AMPS) in HCl. *Synth. Met.* **2005**, *151*, 25–42.
91. Stranick, S. J.; Parikh, A. N.; Allara, D. L.; Weiss, P. S. A New Mechanism for Surface Diffusion: Motion of a Substrate−Adsorbate Complex. *J. Phys. Chem. B* **1994**, *98*, 11136–11142.
92. Yu, M.; Bovet, N.; Satterley, C. J.; Bengió, S.; Lovelock, K. R. J.; Milligan, P. K.; Jones, R. G.; Woodruff, D. P.; Dhanaket, V. True Nature of an Archetypal Self-Assembly System: Mobile Au-Thiolate Species on Au(111). *Phys. Rev. Lett.* **2006**, *97*, 166102-1–166102-4.
93. Moore, A. M.; Mantooth, B. A.; Donhauser, Z. J.; Yao, Y.; Tour, J. M.; Weiss, P. S. Real-Time Measurements of Conductance Switching and Motion of Single Oligo(phenylene ethynylene) Molecules. *J. Am. Chem. Soc.* **2007**, *129*, 10352–10353.
94. Brantley, W. A. Calculated Elastic Constants for Stress Problems Associated with Semiconductor Devices. *J. Appl. Phys.* **1973**, *44*, 534–535.
95. Brough, B.; Northrop, B. H.; Schmidt, J. J.; Tseng, H.-R.; Houk, K. N.; Stoddart, J. F.; Ho, C. M. Evaluation of Synthetic Linear Motor-Molecule Actuation Energetics. *Proc. Natl. Acad. Sci. U.S.A.* **2006**, *103*, 8583–8588.
96. Holland, N. B.; Hugel, T.; Neuert, G.; Cattani-Scholz, A.; Renner, C.; Oesterhelt, D.; Moroder, L.; Seitz, M.; Gaub, H. E. Single Molecule Force Spectroscopy of Azobenzene Polymers: Switching Elasticity of Single Photochromic Macromolecules. *Macromolecules* **2003**, *36*, 2015–2023.